MICROCOPY RESOLUTION TEST CHART
NATIONAL BUREAU OF STANDARDS-1963-A

ADA042901

A New Study of the Outer Zone Electron Environment: A Hazard to CMOS

Space Sciences Laboratory
The Ivan A. Getting Laboratories
The Aerospace Corporation
El Segundo, Calif. 90245

30 June 1977

Interim Report

APPROVED FOR PUBLIC RELEASE:
DISTRIBUTION UNLIMITED

Prepared for

SPACE AND MISSILE SYSTEMS ORGANIZATION
AIR FORCE SYSTEMS COMMAND
Los Angeles Air Force Station
P.O. Box 92960, Worldway Postal Center
Los Angeles, Calif. 90009

DDC
RECEIVED
AUG 15 1977
A

This interim report was submitted by The Aerospace Corporation, El Segundo, CA 90245, under Contract F04701-76-C-0077 with the Space and Missile Systems Organization, Deputy for Advanced Space Programs, P.O. Box 92960, Worldway Postal Center, Los Angeles, CA 90009. It was reviewed and approved for The Aerospace Corporation by G. W. King, Vice President and General Manager, The Ivan A. Getting Laboratories. Lieutenant Dara Batki, SAMSO/YAPT, was the project officer for Advanced Space Programs.

This report has been reviewed by the Information Office (OI) and is releasable to the National Technical Information Service (NTIS). At NTIS, it will be available to the general public, including foreign nations.

This technical report has been reviewed and is approved for publication. Publication of this report does not constitute Air Force approval of the report's findings or conclusions. It is published only for the exchange and stimulation of ideas.

Dara Batki, Lt, USAF
Project Officer

Joseph Gassmann, Major, USAF

FOR THE COMMANDER

LEONARD E. BALTZELL, Col, USAF, Asst.
Deputy for Advanced Space Programs

REPORT DOCUMENTATION PAGE

READ INSTRUCTIONS
BEFORE COMPLETING FORM

1. REPORT NUMBER	2. GOVT ACCESSION NO.	3. RECIPIENT'S CATALOG NUMBER
SAMSO-TR-77-127		

4. TITLE *(and Subtitle)*

A NEW STUDY OF THE OUTER ZONE ELECTRON ENVIRONMENT: A HAZARD TO CMOS.

5. TYPE OF REPORT & PERIOD COVERED

Interim rept.

6. PERFORMING ORG. REPORT NUMBER

TR-0077(2260-20)-9

7. AUTHOR(s)

Alfred L. Vampola, J. Bernard Blake, and George a. Paulikas

8. CONTRACT OR GRANT NUMBER(s)

F04701-76-C-0077

9. PERFORMING ORGANIZATION NAME AND ADDRESS

The Aerospace Corporation
El Segundo, Calif. 90245

10. PROGRAM ELEMENT, PROJECT, TASK AREA & WORK UNIT NUMBERS

11. CONTROLLING OFFICE NAME AND ADDRESS

Space and Missile Systems Organization
Air force Systems Command
Los Angeles, Calif. 90009

12. REPORT DATE

30 June 1977

13. NUMBER OF PAGES

26

14. MONITORING AGENCY NAME & ADDRESS *(if different from Controlling Office)*

27 p.

15. SECURITY CLASS. *(of this report)*

UNCLASSIFIED

15a. DECLASSIFICATION/DOWNGRADING SCHEDULE

16. DISTRIBUTION STATEMENT *(of this Report)*

Approved for public release; distribution unlimited

17. DISTRIBUTION STATEMENT *(of the abstract entered in Block 20, if different from Report)*

18. SUPPLEMENTARY NOTES

19. KEY WORDS *(Continue on reverse side if necessary and identify by block number)*

Radiation Environment
Electron Models
Radiation Damage
Magnetospheric Electrons

20. ABSTRACT *(Continue on reverse side if necessary and identify by block number)*

The Accuracy of the standard model of the magnetospheric energy electron environment, AE4, is examined using in-situ measurements made aboard a number of low altitude spacecraft and synchronous spacecraft. The results indicate that discrepancies exist in the high-energy portion of the model, resulting in errors of up to a factor of 10 in calculated fluxes. Energy transport calculations indicate the dose received by heavily shielded components may be as much as one-and-a-half orders of magnitude greater than would be predicted by the standard model. Methods and data for obtaining a more reliable estimate of dose are furnished.

DD FORM 1473
(FACSIMILE)

407512

CONTENTS

-1-

FIGURES

I. INTRODUCTION

Occasionally, a problem which has been "solved" returns to plague the unwary because the boundary conditions of the problem are subtly changed. The case of radiation hazards to electronic circuitry is an excellent example. In the early and mid-sixties, the remanents of the Starfish nuclear test provided a hostile electron environment in the earth's magnetosphere. The lethal effect of radiation was vividly demonstrated on several satellites in orbit at the time of the test (e.g., TRAAC, Transit-4B). The use of devices with low tolerance to radiation damage was avoided for those satellites which had orbital requirements that took them into the region of the Starfish electrons. However, a good model of the radiation environment was needed for both mission planning and system/subsystem design. The first major model, funded by NASA and produced under the direction of J. I. Vette at The Aerospace Corporation, was the Aerospace Electron Model-1 (AE1) and included data from virtually all electron measuring devices that had been flown on U.S. satellites up to that time (1964). Discrepancies of up to three orders of magnitude occurred between data sets used in that model. Obviously, the model was quite limited in accuracy, at best to perhaps an order of magnitude in the inner radiation zone and perhaps two orders of magnitude in the outer zone (the great variability of the fluxes in the outer zone had not been established at that time). As better data sets became available, the electron and proton models were periodically updated. With the decay of the Starfish electron contribution, the inner zone electron environment became quite benign (relatively few electrons at energies above 1 MeV) and of concern only to sensitive sensor systems; typical electronic components were several orders of magnitude harder than the radiation doses predicted for typical missions in space. But components and missions change. Hence, the return of the problem.

II. THE LOW-ALTITUDE ENVIRONMENT

Figure 1 demonstrates the problem. For a typical polar orbiting satellite, in this case a 450 nmi circular orbit, the radiation dose predicted by the latest NASA electron environment, AE4/AE5, is presented along with some typical component susceptibilities. For typical shielding thicknesses (satellite skin, box walls) of about 75 mils total, the radiation environment was unimportant as long as only bipolar and T^2L circuitry was being used. The advent of large-scale use of CMOS, because of the low tolerance of CMOS to radiation, brought back the radiation damage problem. The problem, of course, extends to all devices with a low threshold for radiation damage (e.g., CCD's, op-amps, and optical couplers).

The lack of margin exhibited by Fig. 1 for CMOS on a typical polar orbit required a more careful analysis of the AE4/AE5 models. The models themselves admit integration errors of factors of 4 to 6 (a fact which is usually ignored by the users of these models). The sources of the error are primarily inconsistencies between data sets and lack of data at high energies. Figure 2 demonstrates the problem. The data sets disagree among themselves by two orders of magnitude. A further problem is that the highest energy point, determined by Explorer 26, comes from an instrument which could not be calibrated with energetic electrons prior to flight.[*] Hence, the high-energy extrapolation of the model is really only a guess, although the best that could be done with the data available.

Because of the severe weight penalty of shielding unnecessarily, a comparison of the AE4/5 models was made with actual data from an energetic electron spectrometer flown on the OV3-3 (1966-70a) satellite in 1966. The result is shown in Fig. 3. The agreement between the model and actual flight data in the inner radiation zone (L < 2.4, where L is McIlwain's parameter and in a dipole corresponds to the geocentric radial distance of the equatorial crossing of the field line) was excellent, $\approx 20\%$. However, a significant discrepancy arises when the outer zone data are included: the model apparently is a "quiet-time" model only. Following large geomagnetic disturbances, significant fluxes of

---

[*] C. E. McIlwain, private communication (1976).
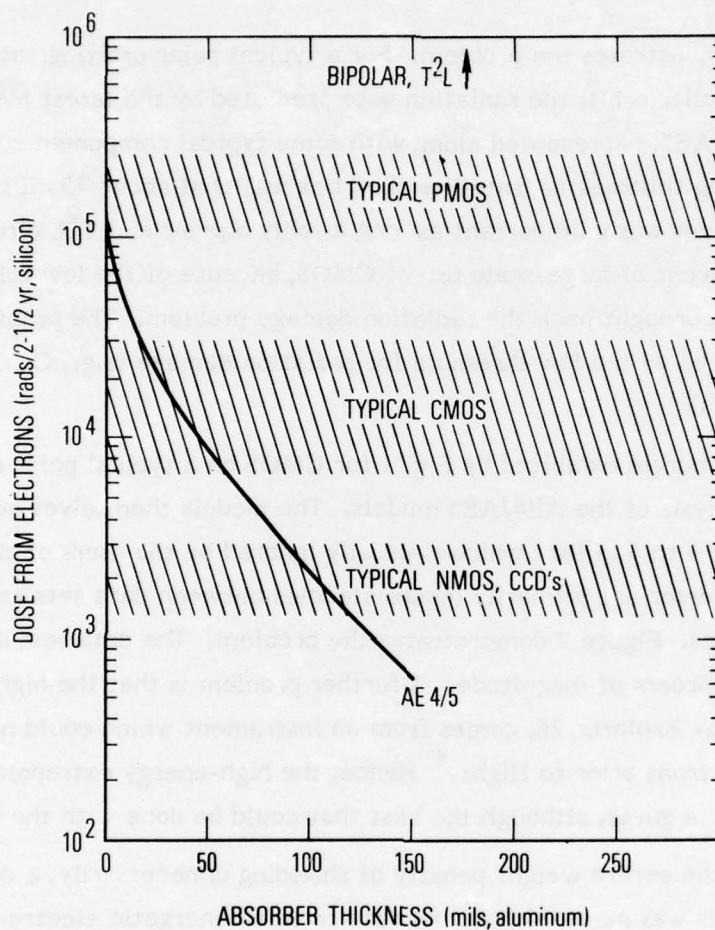
Figure 1. Representative Dose curve Obtained from Calculations Utilizing the AE4/AE5 NASA Electron Environments. Cross-hatched areas represent typical susceptibility levels of various types of electronic components.
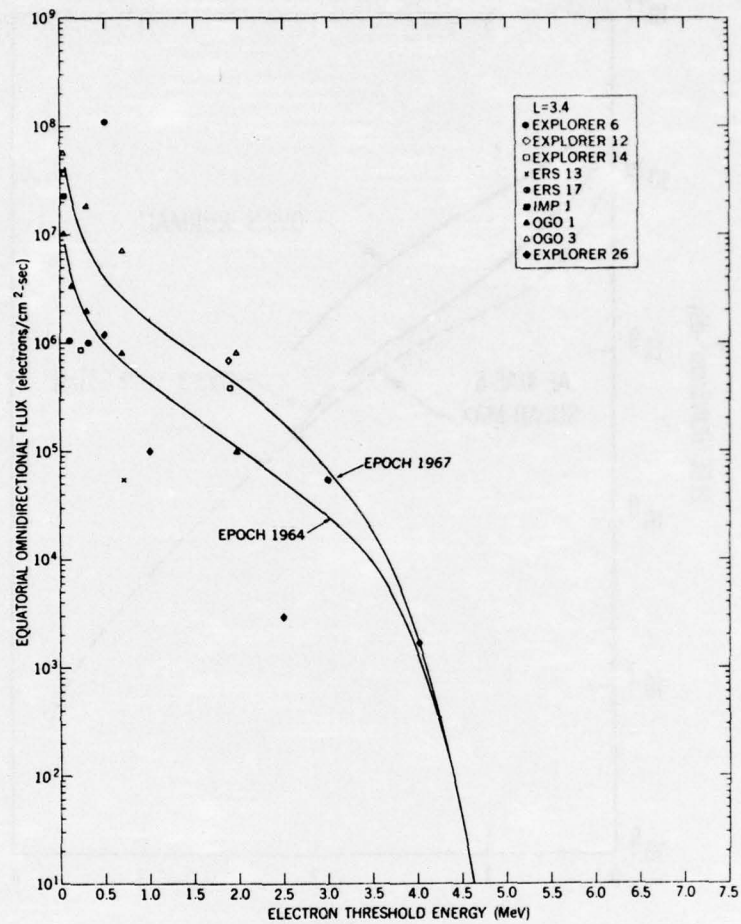
Figure 2. Comparison of AE4 Model spectrum at L = 3.4 with Data Sets Used to develop the Model.[1] The discrepancies are probably partially due to temporal variations.

450 nmi POLAR ORBIT
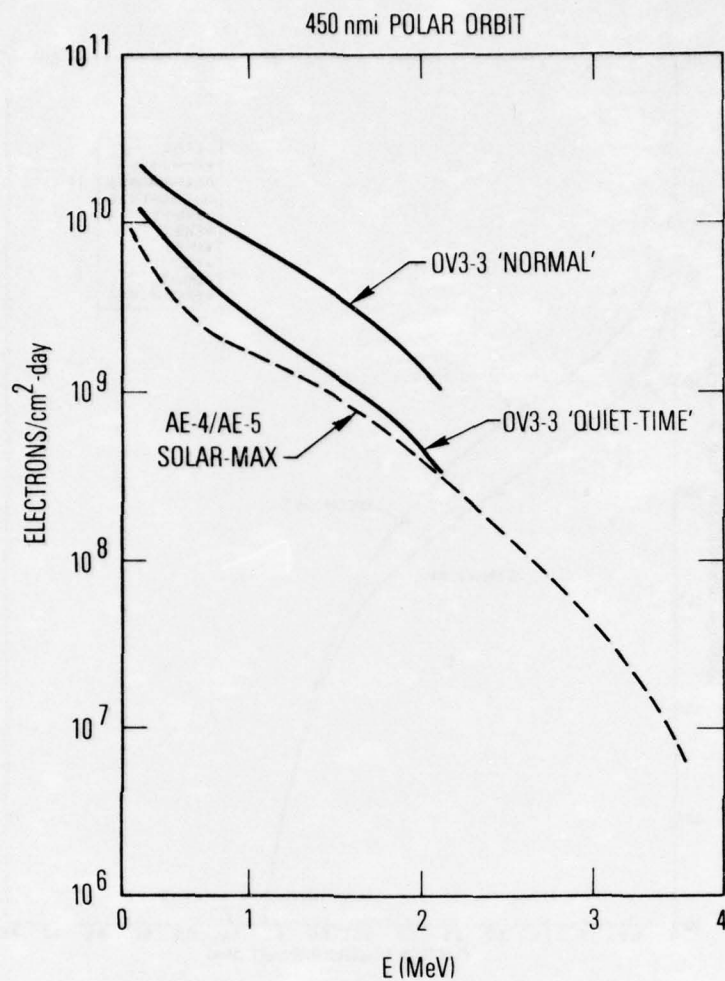
Figure 3. Comparison of the Electron Spectrum in the
AE4 Model with the Results Obtained from
the OV3-3 Satellite for Two Data Sets Sorted
According to Magnetic Storm History. The
"average" spectrum included all data, the "quiet-
time" data included only data preceeded by
magnetically quiet periods. All spectra are
for a typical polar orbit.

energetic electrons appear in the outer zone and persist for some time.[2] These are not adequately modelled in the present NASA models. Since the discrepancy is in the energetic portion of the spectrum(E > 1.5 MeV), the dose effect is much larger than the fluence effect. For the 450 nmi orbit, the fluences predicted by AE4/5 and actually observed by the OV3-3 satellite differed by only a factor of 2. When calculations of dose are made, however, the difference is more like an order of magnitude for thick shields. Figure 4 demonstrates this effect. It also illustrates one of the problems common to both the NASA models and calculations using real data.

When in-situ measurements of the radiation environment are made, only a portion of the spectrum is measured. In the case of the OV3-3 data set, the highest differential energy channel was 2.31 MeV. For all practical purposes, the highest reliable measurement utilized in constructing the NASA models was 1.9 MeV. Above these energies, one must extrapolate. Prior to the use of highly susceptible devices such as CMOS circuitry, the accuracy of the extrapolation was almost totally irrelevant, since the high energy end of the spectrum contributed significant doses only to very heavily shielded components, and for typical missions that dose was orders of magnitude below the damage level.

For the purpose of calculating dose, two extrapolations of the OV3-3 data were made; one extrapolated the dose between 1.5 and 2.3 MeV to 5 MeV and assumed the flux was zero at higher energies; the other was similar but utilized a 10 MeV cutoff. Figure 4 shows the effect of these extrapolations. Also included on Fig. 4 are two data points obtained from a composite measurement of dose made on eight different satellites utilizing approximately a dozen different dosimeters.* The dosimeter data covered the time period 1966-1969. The bulk of the OV3-3 results are available elsewhere.[3]

A final check of the OV3-3 results were made utilizing about 800 hours of data obtained over a period of 15 months during solar minimum on the STP72-1 (1972-76b) satellite. This satellite is in an orbit virtually identical to the 450 nmi orbit and should be an excellent check on the OV3-3 results (which utilized extensive extrapolations to

---

*J. Janni, private communication (1975).
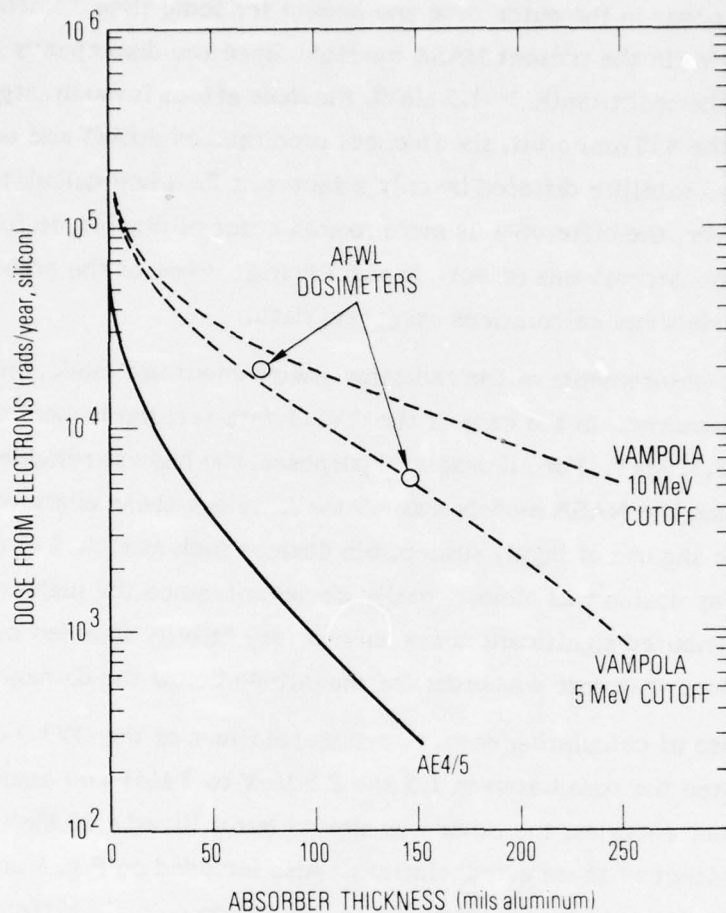
Figure 4. Results of Monte-Carlo Energy Transport
Calculations for the AE4/5 and OV3-3 "Average"
Spectra of Figure 3. In-situ dosimeter measure-
ments are shown for comparison.

low altitude for the 450 nmi result). Figure 5 shows a comparison of the STP72-1 measurements with both "quiet-time" and "average" OV3-3 data. The low-energy portion of the STP72-1 spectrum corresponds to quiet-time data (as would the expected during solar minimum) but the higher energy portion exhibits a harder spectrum than was expected. It is probable that the effects of the August 1972 magnetic storm (one of the largest in the last two decades) on high-energy electrons in the outer zone were still present in the early data from STP72-1 (launched on 2 October 1972).

450 nmi CIRCULAR POLAR ORBIT

Figure 5. Comparison of sTP72-1 Measurements with
the OV3-3 Extrapolations to the 450 nmi
orbit.

-12-

III. THE OUTER ZONE ELECTRON ENVIRONMENT

Because the discrepancy between standard models and the actual environment appears to be limited to the outer zone electron component, it would be u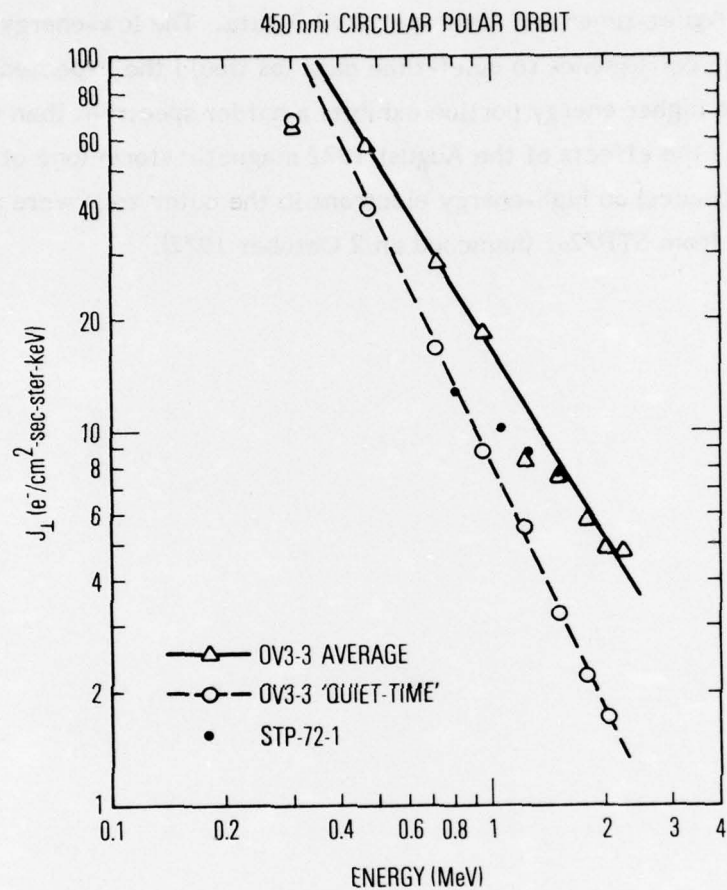seful to examine the morphology of the outer zone electrons in detail, particularly with respect to their response to magnetic storms. Figure 6 presents a series of electron energy spectra taken just prior to, just after, and several weeks after the magnetic storm of 15 May 1969. The data were obtained from magnetic-focusing electron spectrometers on the OV1-19 (1969-25C) spacecraft. The instruments covered the energy range 53 keV to 5.1 MeV in 24 differential energy bands. In Fig. 6, one sees that the major effect of the storm occurs in the >200 keV range, probably because the lower energy electrons are near some self-limiting flux most of the time. After the initial injection/acceleration, the 200 keV to 1 MeV component rapidly returns toward its initial value. However, the >2 MeV component is still increasing two weeks after the storm. Three weeks after the storm the very energetic component has started to decay, but is still about 1½ orders of magnitude greater than prior to the storm. The flux did not return to prestorm levels until several months later. To see how the outer zone electrons respond to magnetic activity over a wide range of energy and L value, we generated Fig. 7 from the OV1-19 data. Three energy bands at four discrete L intervals are plotted for the period March 1969 to February 1970. This period should encompass the peak of the last solar cycle and should be considered representative of solar maximum.

The most dramatic effects are seen in the 0.53 MeV electron channel at L = 3.5. Changes of over 4½ orders of magnitude are observed in response to storms. After the sharp increase, an exponential decrease is observed with a several-day time constant. Note that although all of the storms that produce effects at L = 3.5 in the 0.53 MeV electrons also produce effects in the higher L intervals (further out in the magnetosphere), only two of the storms show significant effects at L = 2.4 (normally considered the outer edge of the inner zone in the NASA models). Also, these effects are relatively modest. The effects at higher energies at L = 2.4 are essentially negligible. The wide variability in the 5.1 MeV flux is partially due to the low statistics associated with counting rates near background.
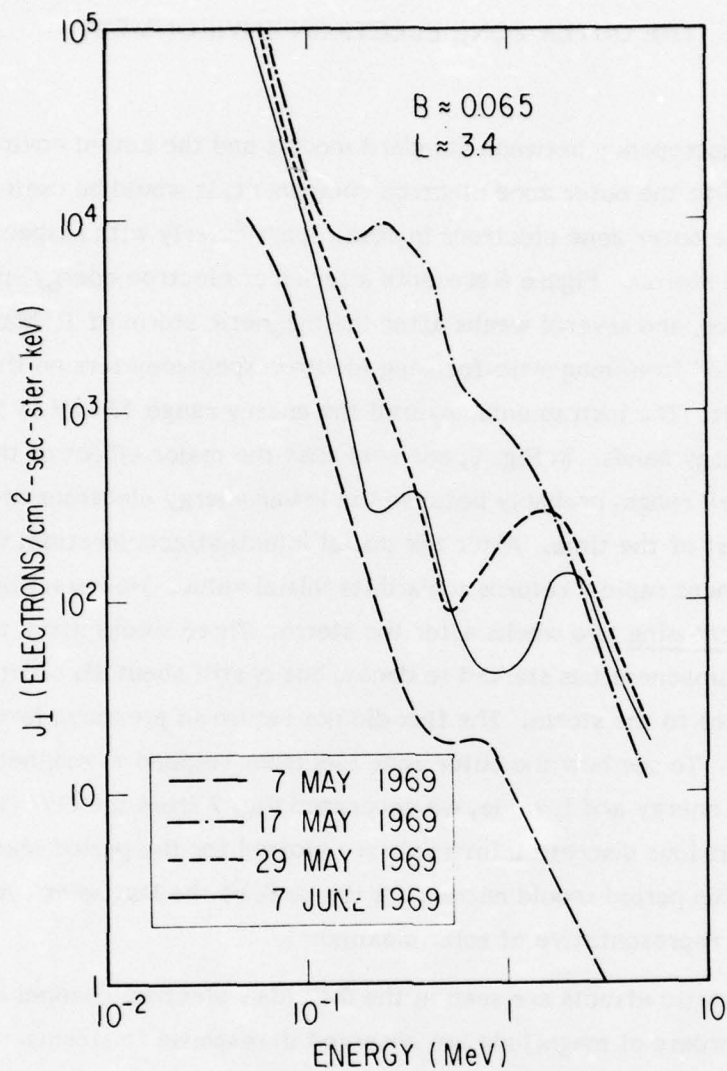
-13-

Figure 6. Energy Spectra from the OV1-19 Satellite
Obtained Preceding and Following the
Magnetic Storm on 15 May 1969.

At higher L intervals, even the high energy electrons respond to relatively minor magnetic field disturbances. The 0.53 MeV electrons at L = 5.5 appear to be limiting at a value of flux lower than that observed in the L = 3.5 interval, and hence do not show dramatic changes, although they do fluctuate rapidly in response to magnetospheric activity. The higher-energy electrons respond to the same activity with about the same magnitude of fluctuations (higher for large storms). However, the response in the interior of the magnetosphere is different from the low energy response. At L = 3.5, the 2.6 MeV and 5.1 MeV electrons respond only to the two largest storms.

All of the data shown in Fig. 7 were obtained at altitudes between 2000 and 4500 km. (Daily averages of the measurements, appropriately normalized to B = 0.05 gauss, are shown.) With a large data base such as this extending to higher energies than have been available previously for modelling purposes, it is appropriate to attempt a refinement of the AE4/5 moels. This we have done. However, first we will show that the relatively low altitude data from OV1-19 are representative of the environment farther up the field lines. In Fig. 8, we show data obtained from OGO-5 near the equator after a magnetic storm in 1968 (data courtesy of H. I. West, Jr.). The inset in Fig. 8 shows the relationship of the OGO-5 data to the 1968 storm and the similar relationship between the data from OV1-19 at low altitude shown in Fig. 6 to its associated magnetic storm. The responses at the equator and lower on the field line show qualitative agreement. All this means is that equilibrium along the field line is achieved in a time span that is short compared to the decay time. It has been previously shown[4] that >300 keV electrons at low altitude come into equilibrium with the electrons at the equator within 0.1 days.

Having demonstrated that the low-altitude data from OV1-19 can be used for modelling the outer zone electron fluxes, we have one further refinement to make. The data of Fig. 7 show two large storm responses. These data were obtained during solar max and can not be considered to be representative of "normal" environments. Since one would expect about one major storm per year on the average, the data for the periods Day 139 to 163 and Day 205 to 235 were deleted from the data set. The resultant average of the data is taken to be an "average" year for the purposes of obtaining a set of coefficients for a temporary modification of AE4.
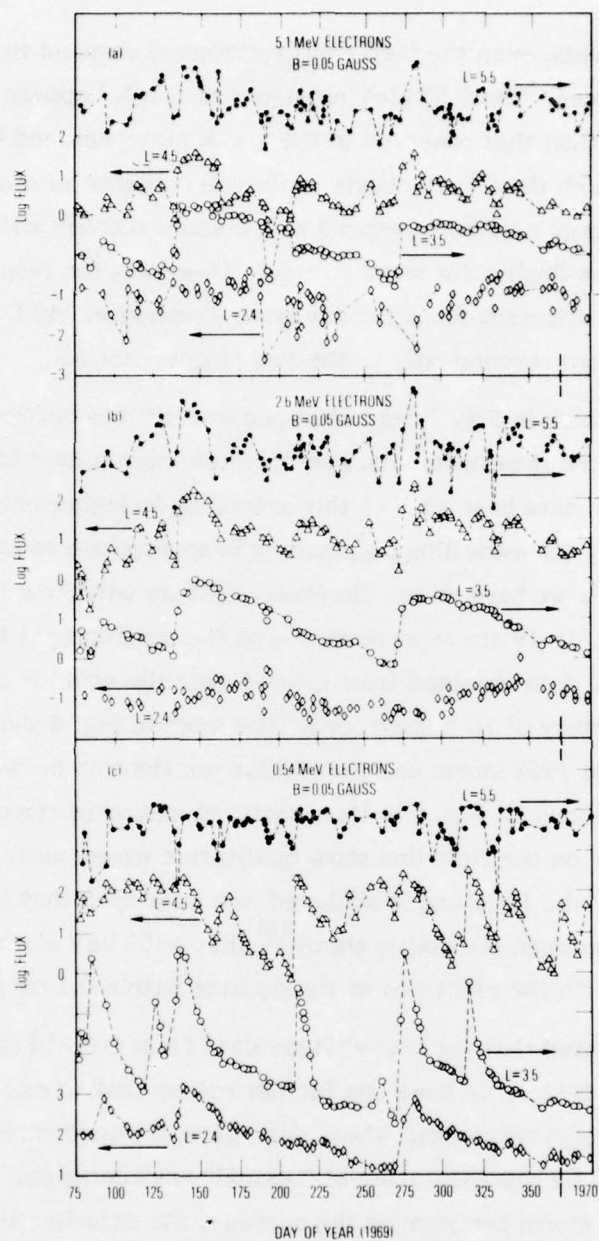
Figure 7. Daily Average Fluxes at 0.53, 2.6, and
5.1 MeV at L Intervals of 2.4, 3.5, 4.5,
and 5.5 for the March 1969 to February
1970 Period. Data are all normalized
to B = .05 gauss. The data were ob-
tained by magnetic electron spectro-
meters on the OV1-19 satellite.

-16-

Figure 8. Energy Spectra from the OV1-19 Satellite
at Low Altitude and the OGO-5 Spacecraft
at High Altitude for Similar Periods after
Major Magnetic Storms. B_o refers to the
equatorial magnetic field value. The inset
details the storms in terms of D_{st}, a mea-
sure of diamagnetic effects on the earth's
field.

Average spectra were obtained for various L values between L = 2.2 and L = 8.0. Since we are attempting to reduce orders of magnitude errors in the high energy portion of the AE4 model to factors of 2 to 4, the da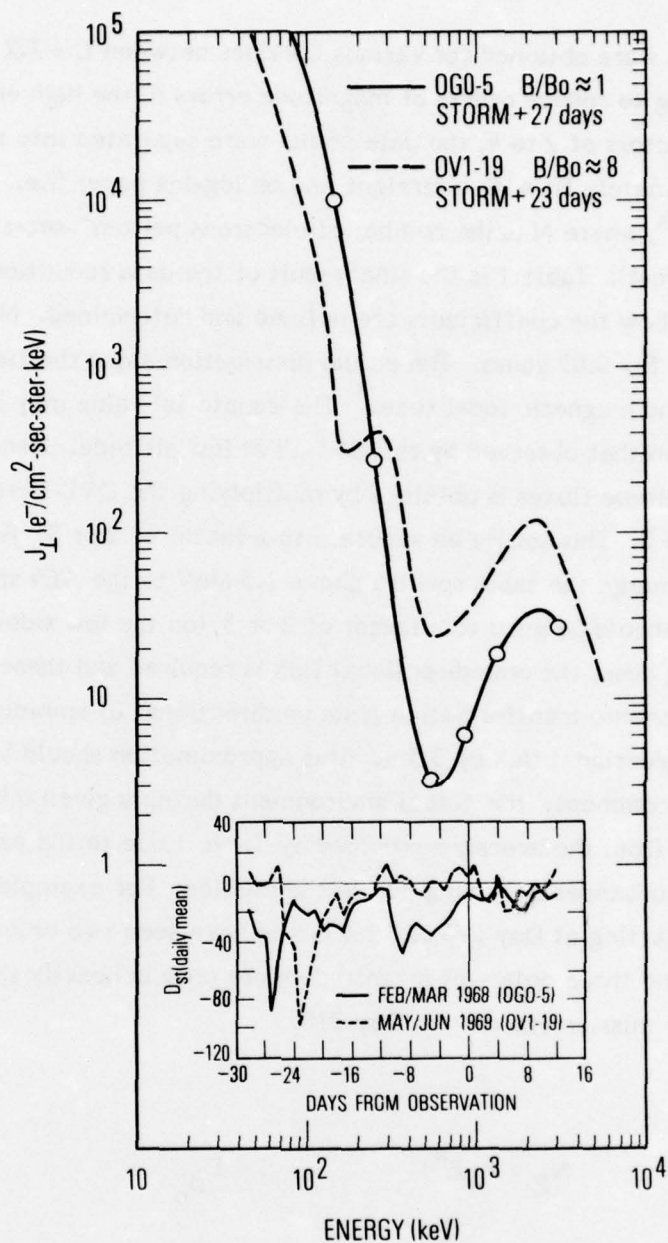ta points were separated into two groups which could be approximately fit with a straight line on log-log paper (i.e., functions of the form $N_E = N_0 E^{-k}$, where N is the number of electrons per cm^2-sec-ster-keV and E is the energy of interest). Table 1 is the final result of the data reduction effort. Figure 9 demonstrates how the coefficients are defined and determined. Note that the data are normalized to B = 0.05 gauss. The actual distribution along the field line is a function of both L and magnetic local time.[*] The equatorial value may be from 6 to 20 times greater than that observed by the OV1-19 at low altitude. Hence, a reasonable assumption for high altitude fluxes is obtained by multiplying the OV1-19 results. (Table 1) by a factor of 8. This should be accurate to a factor of 2 or 3. A second approach that can be used is to merge the table spectra above 1.5 MeV to the AE4 spectra. This will give a result that should be good to a factor of 2 or 3 (on the low side). For the purposes of calculating dose, the omnidirectional flux is required and these values are unidirectional. A reasonable transformation from unidirectional to omnidirectional flux is to multiply the unidirectional flux by $3.5\,\pi$. This approximation should be good to about 15%. One final comment: the actual environment during a given mission can be significantly different from the averages provided by Table 1 due to the particular sequence of magnetospheric disturbances occurring during the mission. For example, a 60-day mission at 15000 km starting at Day 275 of 1969 would have seen two orders of magnitude more energetic flux (and three orders of magnitude more dose in heavily shielded components) than a similar mission starting on Day 210.

Note:

$$N_E = A_1 E^{k_1} \qquad E < E_{B_p}$$

$$\quad = A_2 E^{k_2} \qquad E > E_{B_p}$$

Where N is in electrons/cm^2-sec-ster-keV at B = 0.05 gauss and E is in MeV.

---

[*] H. I. West, Jr., private communication.

Table 1. Outer Zone Energy Spectra Coefficients

| L	A_1	k_1	B_p	A_2	k_2
2.2	850	-1.61	0.36	4.8	- 6.82
2.4	300	-2.17	0.36	0.6	- 8.27
2.6	41	-3.70	0.40	0.026	-10.8
2.8	6.4	-3.98	0.42	0.11	- 6.29
3.0	67	-2.04	0.30	30	- 2.70
3.25	24	-2.42	0.32	13	- 2.86
3.50	105	-1.66	1.10	110	- 2.58
3.75	170	-1.41	1.15	190	- 2.00
4.00	160	-1.62	2.8	480	- 2.66
4.25	195	-1.54	1.10	210	- 2.22
4.50	235	-1.51	1.35	360	- 3.08
4.75	220	-1.54	1.40	470	- 3.74
5.00	235	-1.46	1.00	235	- 3.58
5.25	240	-1.42	0.91	190	- 3.85
5.50	200	-1.43	0.74	95	- 3.88
5.75	120	-1.78	0.75	60	- 4.15
6.00	50	-2.42	1.00	50	- 4.19
6.25	33.5	-2.29	0.54	13.0	- 3.88
6.75	9.2	-2.68	0.70	3.9	- 4.95
7.25	2.15	-3.28	0.90	1.75	- 4.93
7.75	0.53	-3.85	0.80	0.27	- 6.9
8.25	0.19	-3.87	0.80	0.04	-12.2
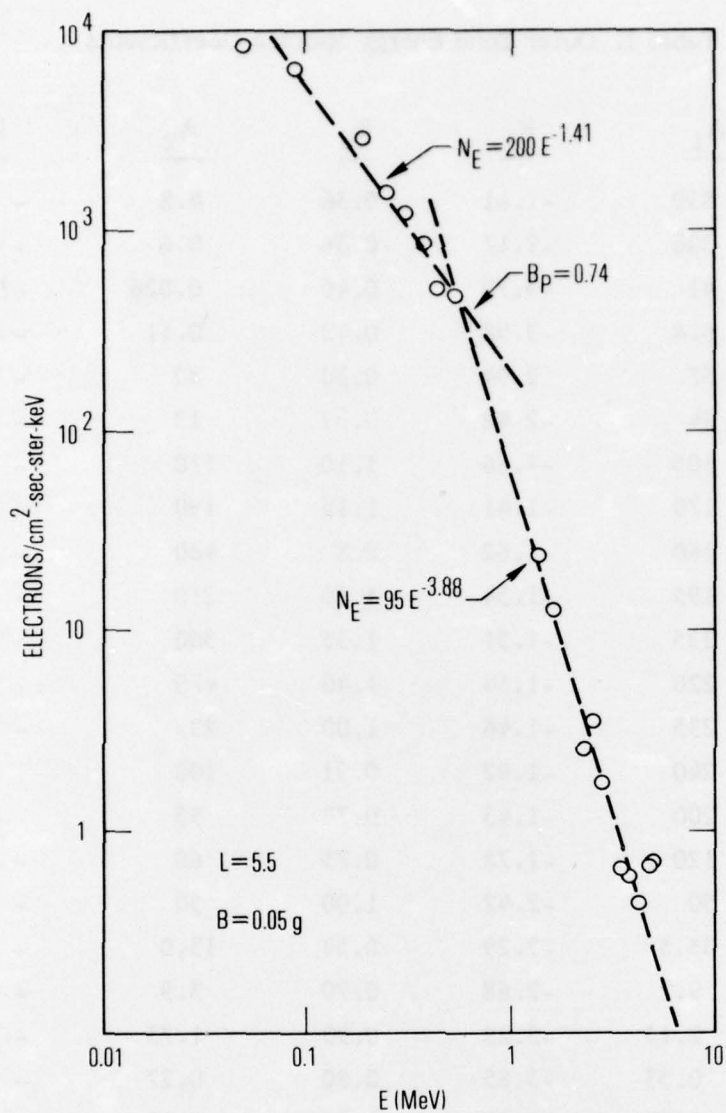
Figure 9. Average spectrum at L = 5.5 Derived from the OV1-19 Data set with the Derivation of the Coefficients Given in Table 1 shown. B_p is the break-point in MeV for the intersection of the spectra.

IV. THE SYNCHRONOUS ENVIRONMENT

The synchronous altitude continues to be a region of exceptional interest because of the great number of satellite missions using and planning to use the geostationary orbit.

The Aerospace experiment aboard ATS-1 (launched December 1966) provided extensive data on the energetic fluxes at synchronous altitude.[5] The Aerospace experiment aboard ATS-6 (launched May 1976) has provided data to compare with the earlier ATS-1 results. The ATS-6 experiment had a channel at 3.9 MeV, whereas the highest energy channel on ATS-1 was 1.9 MeV; however, a direct comparison can be made at the lower energies. It should be remembered that the first ATS-1 data were acquired during 1967, near solar maximum, whereas 1974 was near solar minimum. Furthermore, the two spacecraft were not stationed at the same longitude; ATS-1 is at 150 W, whereas the ATS-6 was acquired when it was at 94°W. Thus, ATS-1 is on the magnetic equator, whereas ATS-6 was at a <u>magnetic</u> latitude ~10°.

The ATS data were treated as follows: for each day of data, hourly averages of the count rates were formed centered on the half hour. The probability $P(F > F_x)$ of observing an integral flux greater than F_x was then calculated for each channel of data according to the formula

$$P(F > F_x) = \frac{\text{Number of Samples with } F > F_x}{\text{total Number of Samples}}$$

In Fig. 10 is shown $P(F > F_x)$ for the three ATS-6 energetic electron channels and the corresponding probability plots obtained from the AE4 model. It can be seen that the environment at the energies under consideration shows a harder spectrum than the AE4 model predicts.

In Fig.11, the effect of the time in the solar cycle is shown in a comparison of ATS-1 data taken in 1967 and 1974. The two ATS-1 data sets acquired at 150°W longitude but separated in time by seven years, indicate that during solar minimum the energetic
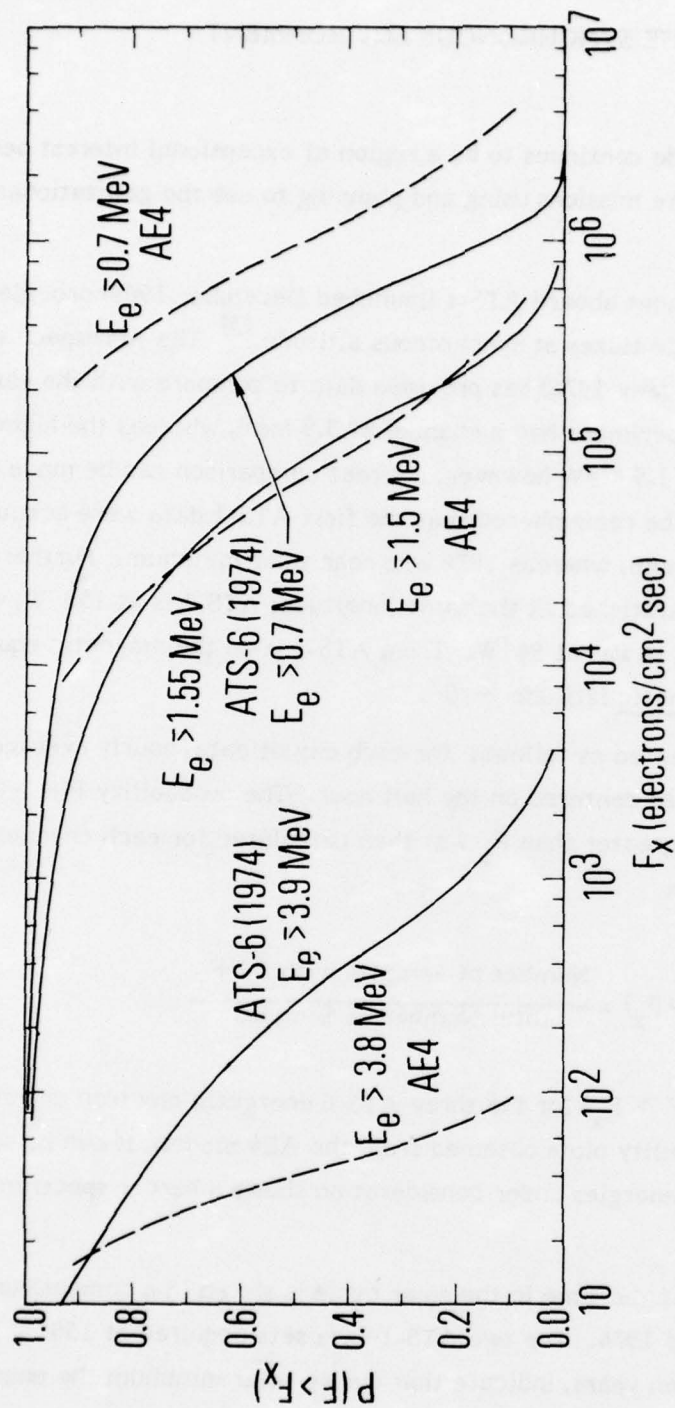
Figure 10. Plots of the Probability P(F > Fₓ) of Observing a Flux of Electrons Greater Than F_x Above Three Integral Thresholds. ATS-6 data (solid curves) and AE4 predictions (dashed curves) are shown. The ATS-6 curves were constructed using 181 days of data obtained between Day 165 (1974) and Day 365 (1974) while ATS-6 was located near 94° W.
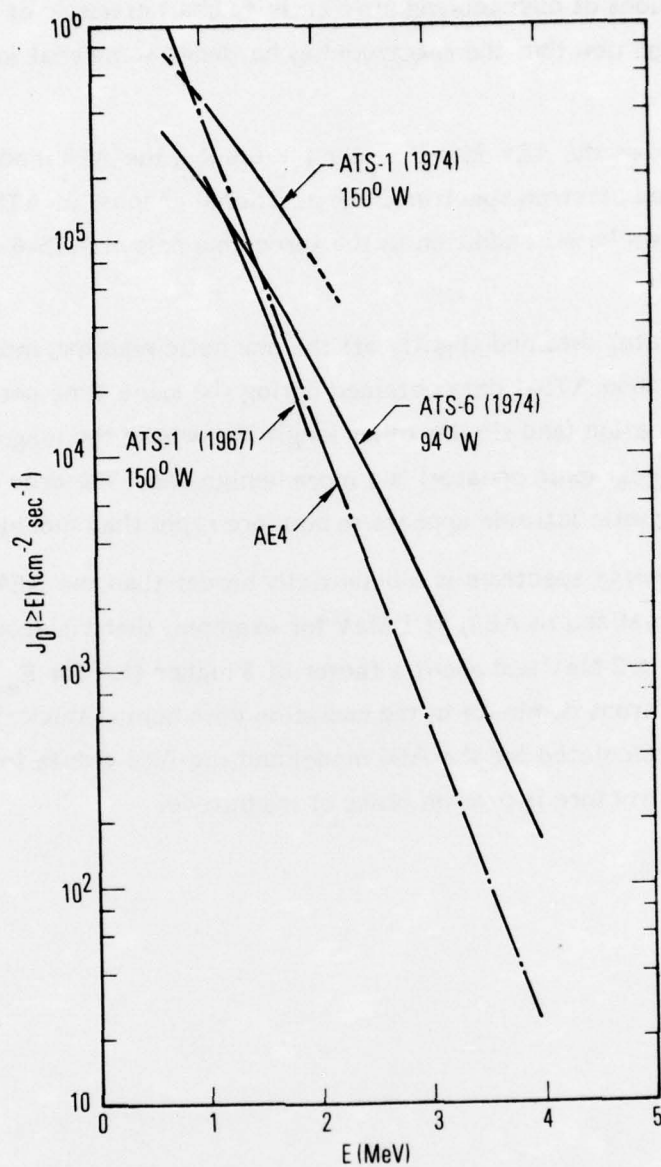
Figure 11. Integral Energy Spectra Constructed
from the $P(F > F_x) = 0.5$ Points for
ATS-6 Data, Two Sets of ATS-1 Data,
and the AE4 Model. (Note that the
$P(F > F_x) = 0.5$ point does <u>not</u> give the
mean flux.)

electron radiation intensity increases about a factor of 2 above that found at the same place during conditions of high geomagnetic activity characteristic of solar maximum. There is also a suggestion that the spectrum has hardened somewhat in going from 1967 to 1974.

Figure 12 shows the AE4 data base for $L = 6.6 \, R_e$, the AE4 model and the ATS-6 time averaged electron spectrum. An additional channel of ATS-6 data, covering 140-600 keV, is shown here in addition to the three channels of ATS-6 data used in Fig.10.

The ATS-6 data, obtained slightly off the magnetic equator, indicated fluxes about a factor of 2 lower than ATS-1 data obtained during the same time period. In other words, the 94° W location (and similar other longitudes where the magnetic equator deviates from the geographic equator) is a more benign one. The drop off of radiation with increasing magnetic latitude appears to be more rapid than models predict.

The ATS-6 energy spectrum is substantially harder than the AE4 model. If the ATS-6 data are normalized to AE4, at 1 MeV for example, there is about a factor of 4 higher flux for $E_e \geq 2$ MeV and about a factor of 8 higher flux for $E_e \geq 3$ MeV. Because the high energy electrons dominate in the radiation dose behind thick shields, the difference between the doses calculated for the AE4 model and the ATS-6 data for parts under typical spacecraft structure is over an order of magnitude.
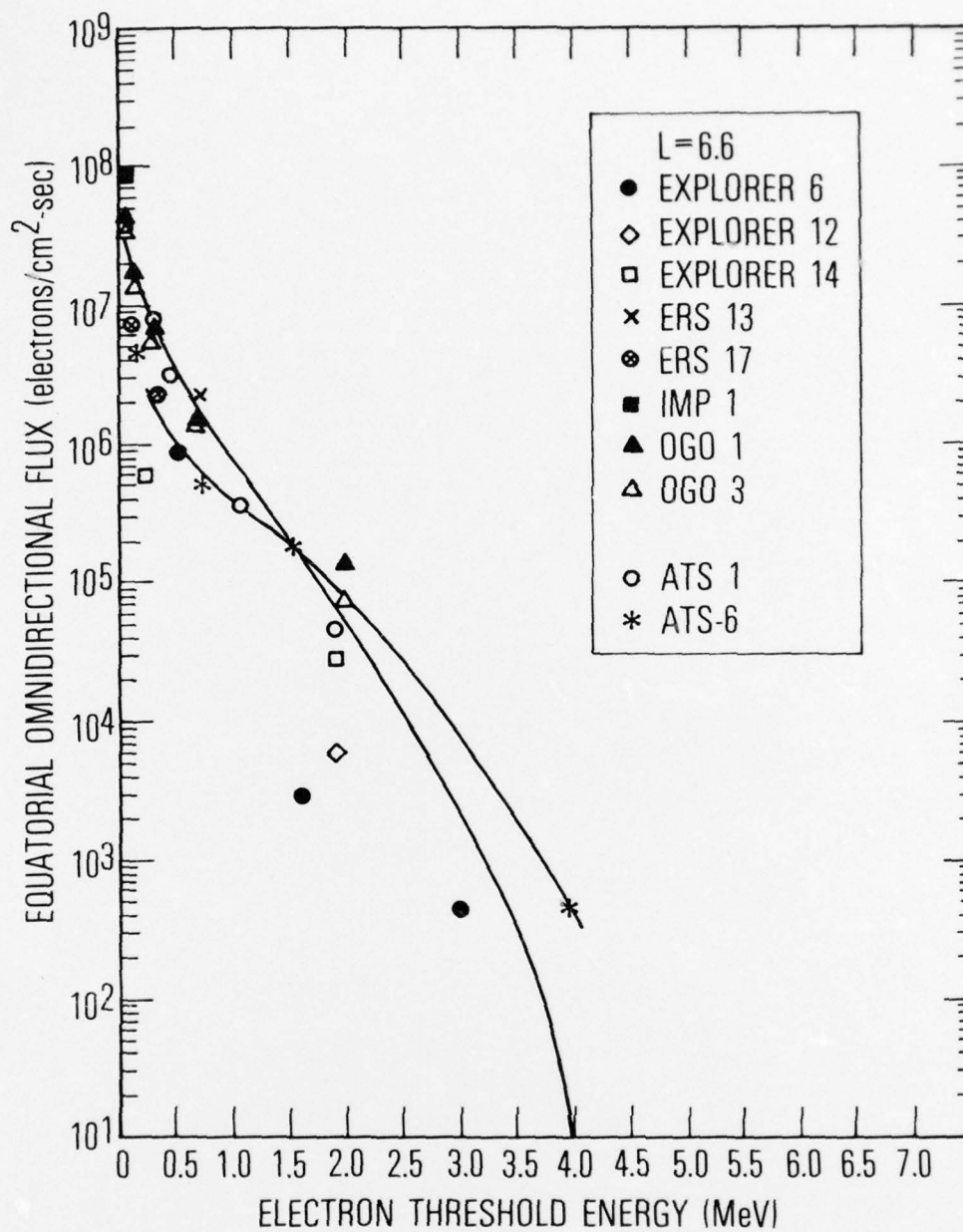
Figure 12. Comparison of ATS-6 with AE4 Data Base.

REFERENCES

1. G. W. Singley and J. I. Vette, "A Model Environment for Outer zone Electrons," National Space Science Data Center, NASA Goodard, NSSDC 72-13.

2. A. L. Vampola, "Natural Variations in the Geomagnetically Trapped Electron Population," in Proceedings of the National Symposium on Natural and Manmade Radiation in Space, E. A. Warman, Ed., NASA TMX-2400, p. 539.

3. A. L. Vampola, "The Energetic Electron Environment in Circular Polar Orbits," TR-0076(6260-20)-2, The Aerospace Corporation, El Segundo, California (15 July 1975).

4. D. J. Williams, J. F. Arens, and L. J. Lanzerotti, "Observations of Trapped Electrons at Low and High Altitudes," J. Geophys. Res., Vol. 73, 1968, p. 5673.

5. G. A. Paulikas an J. B. Blake, "The Particle Environment at the Synchronous Altitude, Models of the Trapped Radiaton Environment. Vol. VII. Long Term Variations," NASA sP-3024 (1971).

PRECEDING PAGE BLANK-Not FILMED

THE IVAN A. GETTING LABORATORIES

The Laboratory Operations of The Aerospace Corporation is conducting experimental and theoretical investigations necessary for the evaluation and application of scientific advances to new military concepts and systems. Versatility and flexibility have been developed to a high degree by the laboratory personnel in dealing with the many problems encountered in the nation's rapidly developing space and missile systems. Expertise in the latest scientific developments is vital to the accomplishment of tasks related to these problems. The laboratories that contribute to this research are:

Aerophysics Laboratory: Launch and reentry aerodynamics, heat transfer, reentry physics, chemical kinetics, structural mechanics, flight dynamics, atmospheric pollution, and high-power gas lasers.

Chemistry and Physics Laboratory: Atmospheric reactions and atmospheric optics, chemical reactions in polluted atmospheres, chemical reactions of excited species in rocket plumes, chemical thermodynamics, plasma and laser-induced reactions, laser chemistry, propulsion chemistry, space vacuum and radiation effects on materials, lubrication and surface phenomena, photosensitive materials and sensors, high precision laser ranging, and the application of physics and chemistry to problems of law enforcement and biomedicine.

Electronics Research Laboratory: Electromagnetic theory, devices, and propagation phenomena, including plasma electromagnetics; quantum electronics, lasers, and electro-optics; communication sciences, applied electronics, semiconducting, superconducting, and crystal device physics, optical and acoustical imaging; atmospheric pollution; millimeter wave and far-infrared technology.

Materials Sciences Laboratory: Development of new materials; metal matrix composites and new forms of carbon; test and evaluation of graphite and ceramics in reentry; spacecraft materials and electronic components in nuclear weapons environment; application of fracture mechanics to stress corrosion and fatigue-induced fractures in structural metals.

Space Sciences Laboratory: Atmospheric and ionospheric physics, radiation from the atmosphere, density and composition of the atmosphere, aurorae and airglow; magnetospheric physics, cosmic rays, generation and propagation of plasma waves in the magnetosphere; solar physics, studies of solar magnetic fields; space astronomy, x-ray astronomy; the effects of nuclear explosions, magnetic storms, and solar activity on the earth's atmosphere, ionosphere, and magnetosphere; the effects of optical, electromagnetic, and particulate radiations in space on space systems.

THE AEROSPACE CORPORATION
El Segundo, California

. . .